



HAL
open science

Early Neoproterozoic (870–820 Ma) amalgamation of the Tarim craton (northwestern China) and the final assembly of Rodinia

Pan Zhao, Jinyou He, Chenglong Deng, Yan Chen, Ross N Mitchell

► **To cite this version:**

Pan Zhao, Jinyou He, Chenglong Deng, Yan Chen, Ross N Mitchell. Early Neoproterozoic (870–820 Ma) amalgamation of the Tarim craton (northwestern China) and the final assembly of Rodinia. *Geology*, 2021, 49 (11), pp.1277-1282. 10.1130/G48837.1 . insu-03286795

HAL Id: insu-03286795

<https://insu.hal.science/insu-03286795>

Submitted on 15 Jul 2021

HAL is a multi-disciplinary open access archive for the deposit and dissemination of scientific research documents, whether they are published or not. The documents may come from teaching and research institutions in France or abroad, or from public or private research centers.

L'archive ouverte pluridisciplinaire **HAL**, est destinée au dépôt et à la diffusion de documents scientifiques de niveau recherche, publiés ou non, émanant des établissements d'enseignement et de recherche français ou étrangers, des laboratoires publics ou privés.

Early Neoproterozoic (870–820 Ma) amalgamation of the Tarim craton (northwestern China) and the final assembly of Rodinia

Pan Zhao^{1*}, Jinyou He², Chenglong Deng¹, Yan Chen³ and Ross N. Mitchell¹

¹State Key Laboratory of Lithospheric Evolution, Institute of Geology and Geophysics, Chinese Academy of Sciences, Beijing 100029, China

²School of Energy Resources, China University of Geosciences, Beijing 100083, China

³Institut des Sciences de la Terre d'Orléans, Université d'Orléans, CNRS/INSU, 45071 Orléans, France

ABSTRACT

In the paleogeographic configuration of the Neoproterozoic supercontinent of Rodinia, the Tarim craton (northwestern China), traditionally seen as a single block, is placed either on the periphery near northern Australia or India or in a central position between Australia and Laurentia. To distinguish between these possibilities, we present here new primary paleomagnetic results from ca. 900 Ma volcanics in the Aksu region of the northwestern Tarim craton. The data reveal a ~28° latitudinal difference between the North Tarim and South Tarim blocks at ca. 900 Ma and constrain the age of amalgamation of the Tarim craton to between 870 and 820 Ma. Combining paleomagnetic poles from Tarim and major cratons of Rodinia with geological evidence, a two-stage orogenic model is proposed for the assembly of Rodinia. Late Mesoproterozoic orogenesis (1.3–1.0 Ga) led to the assembly of Australia–East Antarctica, Baltica, Umkondia, South Tarim, and Cathaysia with Laurentia, forming the core of Rodinia. Thereafter, the Jiangnan–Central Tarim Ocean separating North Tarim and Yangtze from South Tarim and Cathaysia was closed before ca. 820 Ma. This second Jiangnan–Central Tarim orogeny caused nearly coeval amalgamation of the peripheral Tarim and South China cratons by the welding of North Tarim and Yangtze to South Tarim and Cathaysia, respectively. The supercontinent of Rodinia was thus assembled by two orogenic phases separated by ~200 m.y.

INTRODUCTION

Since Hoffman's (1991) proposal of a paleogeographic configuration of the Rodinia supercontinent, there have been many investigations of continents, cratons, and blocks aimed at deducing their relative positions in different models of the Neoproterozoic supercontinent (Fig. 1; e.g., Dalziel, 1997; Pisarevsky et al., 2003; Li et al., 2008; Evans, 2013; Merdith et al., 2021). Most Rodinia models place Laurentia in a central position due to the surrounding Neoproterozoic passive margins, where it is surrounded by Baltica, Africa, Amazonia, Antarctica, Australia, and Siberia, with Asian cratons (e.g., South China and Tarim) on the periphery near Antarctica–Australia (Hoffman, 1991; Pisarevsky et al., 2003; Evans, 2013). However, the initial placement of Asian cratons at the periphery of Rodinia was challenged as new paleomagnetic and geological data were reported from each cra-

ton (e.g., Pisarevsky et al., 2003; Li et al., 2008; Merdith et al., 2021). Li et al. (1995) proposed a “missing link” model for Rodinia that places South China at the heart of Rodinia between Laurentia and Australia (Fig. 1D). Conversely, in the model of Merdith et al. (2021), South China is situated at a high paleolatitude and far away from Rodinia during the early Neoproterozoic (Fig. 1F). Recently, Wen et al. (2018) located Tarim between Laurentia and Australia and proposed a connection to South China based on a newly reported 890–870 Ma paleomagnetic pole from southern Tarim. This wide range of competing models highlights the uncertainties surrounding the history of the Asian cratons in the configuration and assembly of Rodinia.

The Tarim craton (northwestern China) has been considered to have been a rigid craton since at least the Mesoproterozoic (Zhang et al., 2013). However, the identification of an east-west aeromagnetic anomaly in central Tarim (He et al., 2011) and the presence of Paleopro-

terozoic (1968–1895 Ma) and Neoproterozoic (933–891 Ma; Fig. 2) granitoids within this belt (Li et al., 2005; Xu et al., 2013; Wu et al., 2020) has led to the proposal of a collision of the North Tarim and South Tarim blocks along the Central Tarim suture at either of these ages (Xu et al., 2013; Wu et al., 2020). However, current evidence to support these hypotheses is insufficient to discriminate between Paleoproterozoic and Neoproterozoic amalgamations. In order to test the Neoproterozoic collision of North Tarim and South Tarim and further constrain its paleogeographic location during the final assembly of Rodinia, we conducted a paleomagnetic study on the newly identified ca. 900 Ma volcanics of the Aksu region of northwestern Tarim (He et al., 2019). The new data enable us to constrain an amalgamation of the Tarim craton to between 870 and 820 Ma through parallel subduction belts on the periphery of Rodinia and thus establish the age of final assembly of the Neoproterozoic supercontinent.

GEOLOGICAL SETTING OF THE QIGELEKEKUOTAN VOLCANICS

The Tarim craton is bounded by the Tianshan mountains to the north, the western Kunlun Mountains to the southwest, and the Altyn Tagh fault to the southeast (Fig. 2A). The basement rocks are composed of Archean gneisses and Paleoproterozoic–Mesoproterozoic metasedimentary and metavolcanic rocks that are unconformably overlain by Neoproterozoic–Phanerozoic sedimentary rocks (Zhang et al., 2013). In the Aksu region of northwestern Tarim, the newly identified Qigelekekuotan volcanics are dated by laser ablation–inductively coupled plasma–mass spectrometry (LA-ICPMS) U–Pb ages from zircons to between 909 and 903 Ma (Fig. 2C; He et al., 2019). The Qigelekekuotan volcanics, interpreted as volcanic arc in origin

*E-mail: panzhao@mail.iggcas.ac.cn

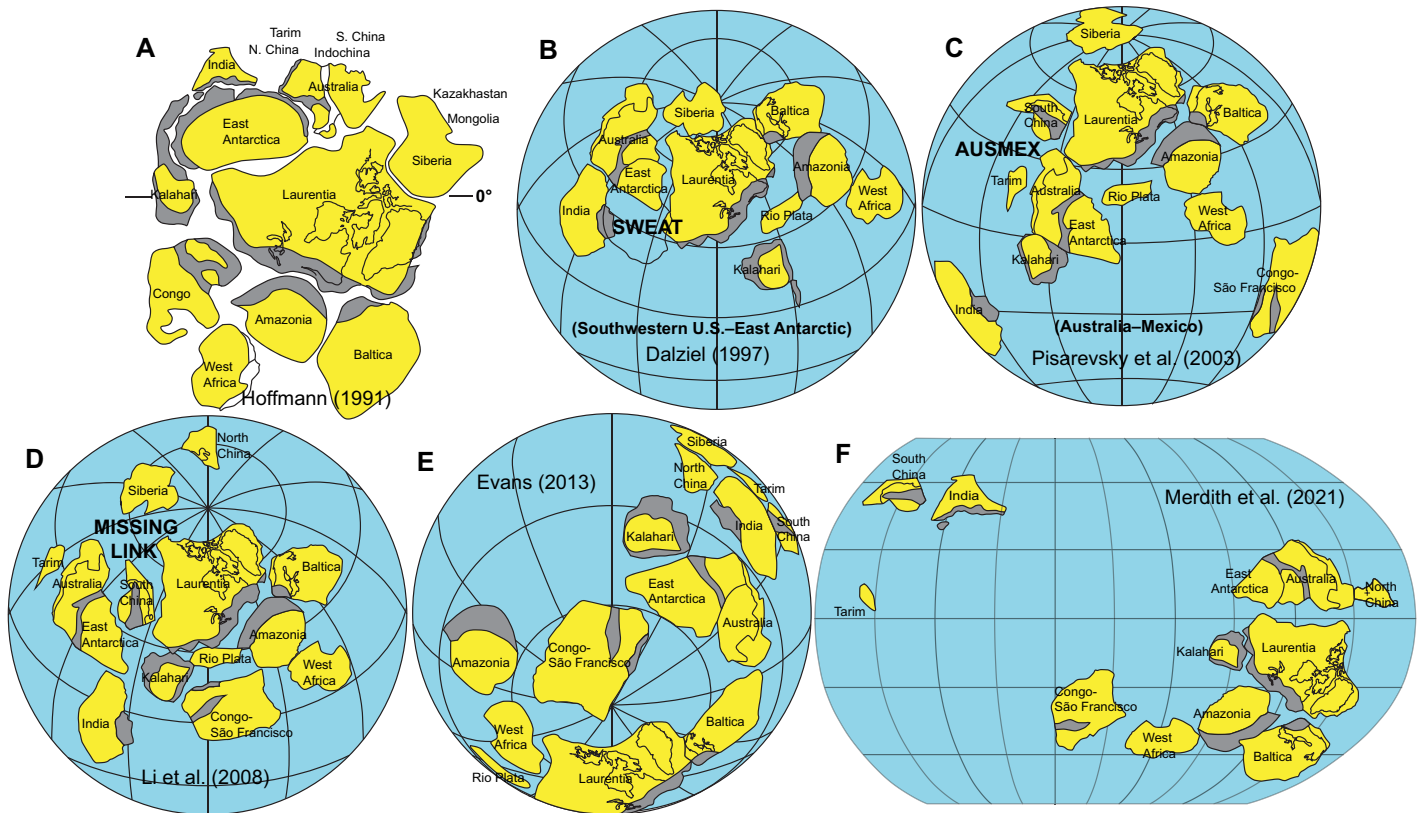


Figure 1. Six representative models for Rodinia reconstruction. Blocks (in yellow) and Rodinia-forming orogens (gray) are shown. (A) The Rodinia supercontinent at ca. 700 Ma after Hoffmann (1991). (B–E) Reconstructions of Rodinia showing in modern North American coordinates, after Dalziel (1997), Pisarevsky et al. (2003), Li et al. (2008), and Evans (2013). (F) Rodinia supercontinent at ca. 900 Ma, after Merdith et al. (2021).

(He et al., 2019), are unconformably overlain by clastic rocks of the Cryogenian Qiaoenbrak Group and the Ediacaran Sugetbrak Formation (Fig. 2B). The Qigelekekuotan volcanics are mainly composed of green- and purple-colored andesite, tuff, and red-colored rhyolite interlayers that define the volcanostratigraphic bedding for paleomagnetic paleohorizontal (Fig. 2C; Fig. S1 in the Supplemental Material¹).

NEW CA. 900 MA PALEOMAGNETIC POLE FROM NORTH TARIM

In total, 21 paleomagnetic sites were sampled along a 1.5 km cross section of the Qigelekekuotan volcanics (Fig. 2C). Standard paleomagnetic sampling, laboratory, and analytical methods were used and are detailed in the Supplemental Material. Rock magnetic investigations reveal magnetite and hematite as the main magnetic carriers (Figs. 3A and 3B; Fig. S2). Two magnetic components were isolated from most specimens by stepwise thermal demagnetization (Figs. 3C and 3D). The low-temperature component yields a mean direction close to that

of the present local field, and thus represents a viscous and/or a weathering overprint. After removal of the overprint, the high-temperature component exhibits both normal and reversed polarities (Figs. 3C and 3D), where such characteristic remanent magnetizations were successfully isolated from 15 of 21 sites (Table S1 in the Supplemental Material). A mean direction was calculated with the 15 sites at declination/inclination (D/I) = 155.2°/47.5°, k (precision parameter) = 11.6, α_{95} (95% confidence for spherical distribution) = 11.7° before tilt correction, and D/I = 205.2°/64.0°, k = 24.4, α_{95} = 7.9° after tilt correction (Figs. 3E and 3F; Table S1). The direction-correction (DC) fold test (Enkin, 2003) yields a positive result with a DC slope at 97.0% ± 21.5% untilting (Fig. 3G). The parametric simulation fold test (Watson and Enkin, 1993) yields an optimum degree of untilting at 96.0% ± 12.2% (Fig. 3H), also indicating a positive fold test. Given that the gently titled Cryogenian Qiaoenbrak Group unconformably overlies the Qigelekekuotan volcanics (Fig. 2C; Fig. S1), the age of folding of the Qigelekekuotan volcanics should be older than the ca. 730 Ma age of the Qiaoenbrak Group. The reversal test (McFadden and McElhinny, 1990) is indeterminate due to the presence of only one opposite-polarity site. Nonetheless, the positive fold tests argue for a primary magnetic rema-

nence. Therefore, a ca. 900 Ma paleomagnetic pole was calculated for North Tarim at 0.3°N, 63.8°E, and A_{95} (95% confidence for spherical distribution) = 11.8° with a corresponding paleolatitude of 47.0°N ± 11.8°. According to the paleomagnetic reliability criteria of Meert et al. (2020), our new pole scores a six (out of seven), indicating a reliable pole. Meanwhile, this pole differs from younger Tarim poles, also consistent with a primary origin (Table S2; Fig. 4A).

AMALGAMATION OF TARIM

The Precambrian crustal evolution of the Tarim craton remains largely unknown because most of it is covered by the Taklamakan Desert. There is ongoing debate as to whether the Tarim craton became a rigid craton in Paleoproterozoic (Wu et al., 2020) or Neoproterozoic time (Xu et al., 2013). Based on the discovery of ca. 1.9 Ga magmatic rocks in the Central Tarim suture, a Paleoproterozoic welding of North Tarim and South Tarim was suggested (Wu et al., 2020). Compiling information on Proterozoic magmatism across the craton, Xu et al. (2013) proposed a separate evolution of North Tarim and South Tarim during the Mesoproterozoic and the final amalgamation of these two terranes between 1.0 and 0.82 Ga.

However, neither the age nor the kinematics of the final collision of North Tarim and South

¹Supplemental Material. Supplemental text, Figures S1 and S2, and Tables S1–S3. Please visit <https://doi.org/10.1130/GEOL.S.14810538> to access the supplemental material, and contact editing@geosociety.org with any questions.

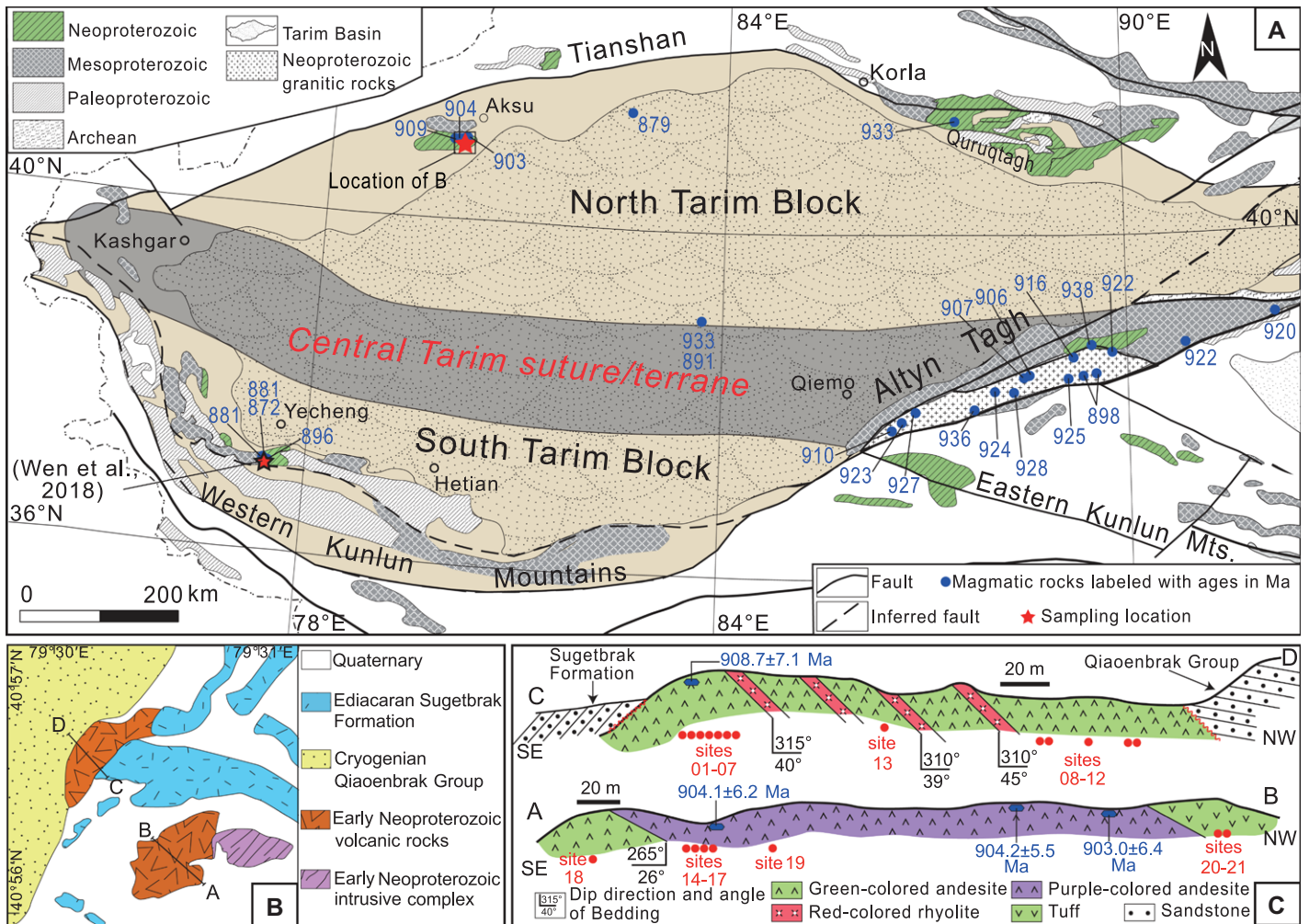


Figure 2. (A) Sketch map of the Tarim craton showing Precambrian geology and surrounding orogens with the Central Tarim orogenic suture and extensive early Neoproterozoic (940–870 Ma) arc magmatism (after Xu et al., 2013; He et al., 2019). **(B)** Simplified geological map of the sampling region in the Aksu region including locations of cross sections of sampling locations. **(C)** Cross sections showing rock types, volcanostratigraphic bedding, reported zircon U-Pb ages, and paleomagnetic sampling locations.

Tarim is constrained. Our new paleomagnetic pole and paleolatitude of $47.0^{\circ}\text{N} \pm 11.8^{\circ}$ at ca. 900 Ma for the Qigelekekuotan volcanics of North Tarim provide key constraints for this problem. Wen et al. (2018) reported an 890–870 Ma paleomagnetic pole from the Sajaizitige Group volcanics in South Tarim at $23.5^{\circ}\text{S}/37.0^{\circ}\text{E}$, $A_{95} = 11.3^{\circ}$, with a corresponding paleolatitude of $18.6^{\circ}\text{N} \pm 11.3^{\circ}$. Even with a combined uncertainty of the two paleolatitudes of 23.1° , the large latitudinal discrepancy (28.4°) between North Tarim and South Tarim is statistically significant and indicates that a wide Central Tarim Ocean separated the two blocks between 900 and 870 Ma. Alternatively, a unified Tarim craton drifting rapidly would have required an unprecedented fast tectonic motion of ~ 24 cm/yr. Even stretching age uncertainties yields a rate (8 cm/yr) that is faster than that of any continental plate today. Considering that this separation between North Tarim and South Tarim based on paleolatitude alone is a conservative estimate, we deem the separated North

Tarim and South Tarim scenario more tectonically plausible. Because no ophiolite mélangé or high-pressure metamorphic rocks have yet been found in the Central Tarim suture zone, it is impossible to define the exact age of final collision. However, subsequent mantle plume-related mafic magmatism exhibited across the craton from 820 to 800 Ma must postdate the amalgamation of North Tarim and South Tarim (Zhu et al., 2011; Xu et al., 2013) as well as implies a rather sudden transition to rifting within the newly formed craton. Therefore, the final amalgamation of Tarim must have occurred between 870 and 820 Ma.

THE FINAL ASSEMBLY OF RODINIA

In the first paleogeographic reconstruction of Rodinia, Asian cratons, such as Tarim and South China, were placed along the northern margin of Rodinia near Australia (Hoffman, 1991). Paleomagnetic results have supported this hypothesis and highlighted long-term Australia–Tarim (Li et al., 2008; Zhao et al., 2014)

and Australia–South China connections (Yang et al., 2004). Based on the early Neoproterozoic Jiangnan orogeny between the Yangtze and Cathaysia blocks, Li et al. (1995) proposed a “missing link” model for Rodinia that placed South China in the center in between Laurentia and Australia. However, U-Pb ages for the Jiangnan orogeny of 860–820 Ma (Zhao et al., 2011; Cawood et al., 2018; Lin et al., 2018; Yan et al., 2019; Yao et al., 2019) are much younger than that of Grenvillian orogenesis. Furthermore, evidence for Neoproterozoic arc magmatism along the northern margin of the Yangtze block, indicating an active plate margin, requires that South China was located along the periphery of Rodinia during the period between 990 and 820 Ma (Cawood et al., 2013, 2018; Wang et al., 2013). Geological evidence for a peripheral position of South China in Rodinia (Zhao et al., 2011; Cawood et al., 2013) is also supported by recent paleomagnetic reconstructions (Jing et al., 2020). Wen et al. (2017, 2018) expanded the “miss-

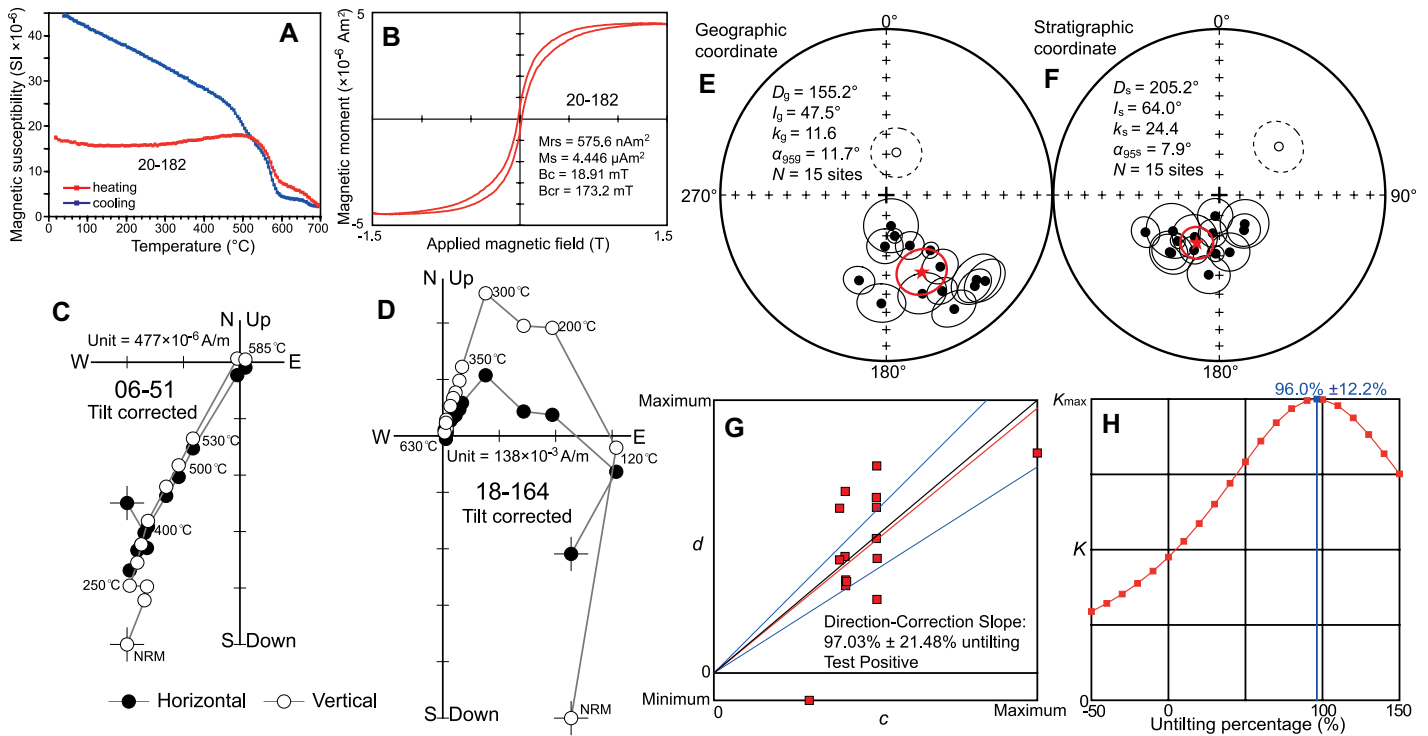


Figure 3. Paleomagnetic and rock magnetic results from Qigelekekuotan volcanics (Tarim craton). (A,B) Thermomagnetic curve of magnetic susceptibility (A) and magnetic hysteresis loop (B). *Mrs*—saturation remanent magnetization; *Ms*—saturation magnetization; *Bc*—coercivity; *Bcr*—coercivity of remanence. (C,D) Orthogonal projections of representative stepwise demagnetization and corresponding directions plotted in tilt-corrected coordinates. NRM—natural remanent magnetization. (E,F) Equal-area projections of 15 site-mean directions in geographic (E) and stratigraphic (F) coordinates with filled (open) circles representing normal (reversed) polarities. Ellipses represent 95% confidence of the site-mean direction. (G,H) Positive fold tests for remanence of Qigelekekuotan volcanics. *K*—precision parameter; *K_{max}*—maximum value of precision parameter.

ing link” model and put Tarim together with South China between Australia and Laurentia. In this new model, the collision between South Tarim–Australia and North Tarim–Laurentia was completed at least by ca. 900–880 Ma, followed by subsequent, peripheral Rodinia assembly. However, Tarim as a missing link has been challenged by the identification of Neoproterozoic oceanic subduction along the northern margin of Tarim, evidence of which includes the ca. 700 Ma Aksu blueschist, and 820–790 Ma high-pressure granulites that cannot be explained with Tarim in a central Rodinia position (Song and Li, 2019). Our new paleomagnetic data indicate separate tectonic histories of North Tarim and South Tarim prior to Rodinia assembly and the existence of a wide Central Tarim Ocean (~28° latitudinal distance) between them at 900–870 Ma. A peripheral position of Tarim in Rodinia can accommodate subduction of such a wide ocean. Magmatism constraining the collision between North Tarim and South Tarim between 870 and 820 Ma is broadly coeval with the Jiangnan orogeny between the Yangtze and Cathaysia blocks of the South China craton.

Incorporating paleomagnetic data from Tarim and South China and other major cratons of Rodinia (Table S3) with geological evidence, we propose a kinematic solution for the

final assembly of Rodinia along its northern margin (Figs. 4B and 4C). Earliest Rodinia orogenesis aggregated Kalahari, Amazonia, Congo, and other cratons of southern Rodinia in a configuration that has been referred to as “Umkondia” for its assembly by the time of the ca. 1.1 Ga Umkondo large igneous province (Choudhary et al., 2019). During Grenvillian orogenesis (1.3–1.0 Ga), Australia–East Antarctica, Amazonia (of Umkondia), and Baltica assembled along the western, eastern, and northeastern margins of Laurentia, respectively, thus forming the core of Rodinia (Hoffman, 1991; Li et al., 2008). It was also during this time that Cathaysia and South Tarim, potentially near or connected to each other, likely joined Rodinia north of Australia based on the identification of 1.3–1.0 Ga high-grade metamorphism (Spencer et al., 2017) and paleomagnetic reconstructions (Fig. 4B; Evans, 2013; Li et al., 2008; Wen et al., 2018). In the early Neoproterozoic, however, neither South China nor Tarim were yet amalgamated as cratons. Cathaysia and South Tarim were situated proximal to the newly formed core of Rodinia (Fig. 4B; Cawood et al., 2013; Wen et al., 2018). On the other hand, Yangtze and North Tarim both occupied relatively high paleolatitudes to the north of Rodinia and were separated from their southern counterparts by

the Jiangnan–Central Tarim Ocean (Fig. 4B). To accommodate the wide Jiangnan–Central Tarim Ocean, it is reasonable to place these blocks along the periphery, rather than in the center, of Rodinia.

Closure of the Jiangnan–Central Tarim Ocean occurred between 870 and 820 Ma and was achieved by the collisions of Yangtze and Cathaysia in the Jiangnan orogeny and of North Tarim and South Tarim in the Central Tarim suturing event (Fig. 4C). Evidence for the subduction of the Jiangnan–Central Tarim Ocean is found in Neoproterozoic arc magmatism along multiple active margins of the Yangtze, Cathaysia, and North Tarim blocks (Fig. 3B; Zhao et al., 2011; Yao et al., 2019). The polarity of this subduction zone or whether two-sided subduction was involved is unresolved (Fig. 4B) due to limited data for the Central Tarim suture and competing models for the collision between Yangtze and Cathaysia that range from northwestward subduction beneath Yangtze (Zhao et al., 2011; Yan et al., 2019) to southeastward subduction beneath Cathaysia (Cawood et al., 2013; Yao et al., 2019) to two-sided subduction beneath both Yangtze and Cathaysia (Zhao, 2015). In any case, there is evidence that after peripheral accretion of Yangtze and North Tarim, a circum-Rodinia subduction girdle with arc magmatism developed along

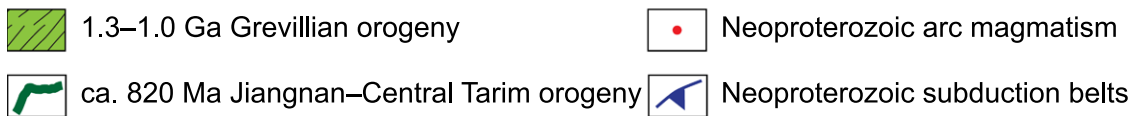
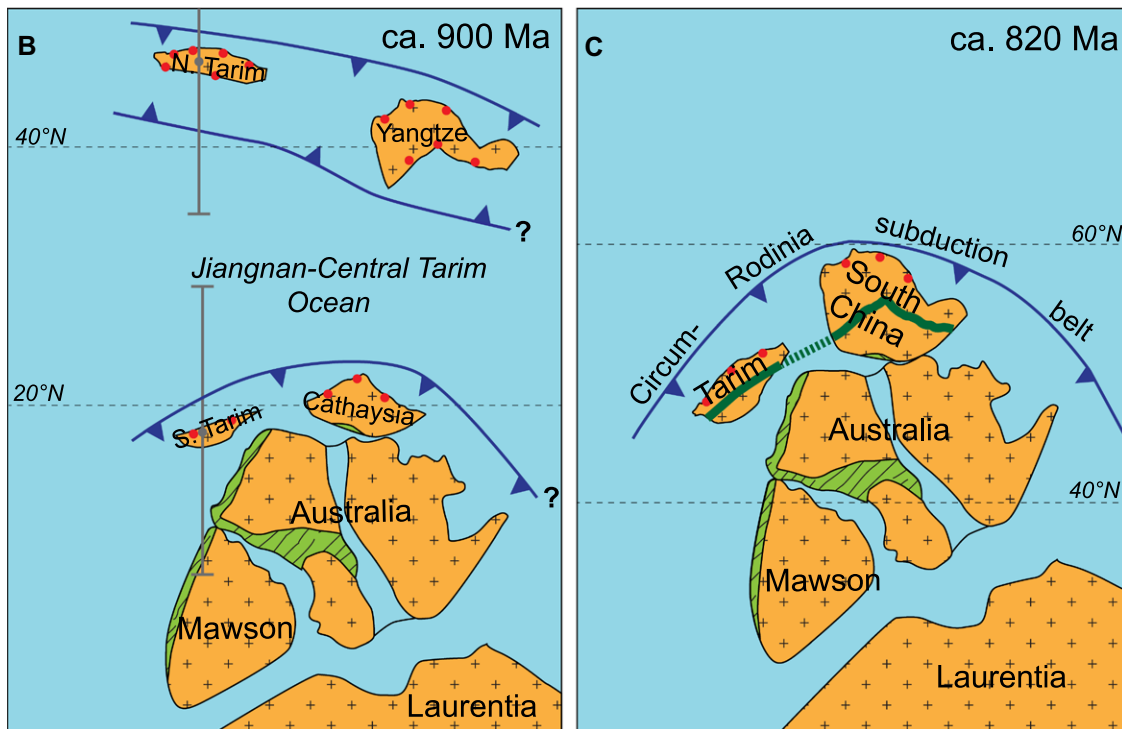
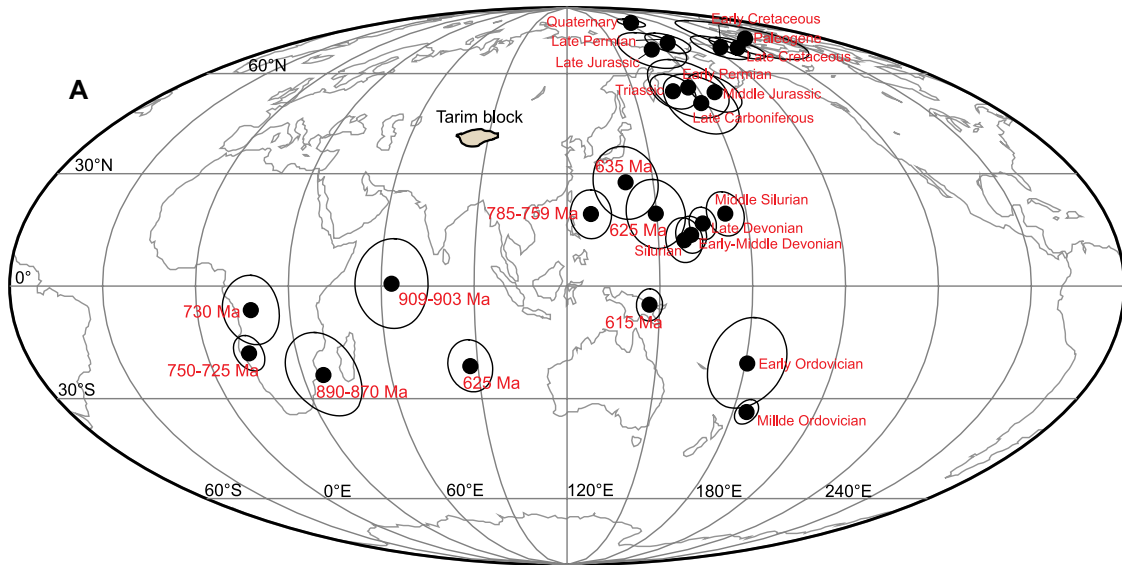


Figure 4. Paleopoles and paleogeography. (A) Paleopoles from the Tarim craton (Table S3 [see footnote 1]). (B,C) Paleogeographic reconstructions of northern Rodinia at ca. 900 Ma (B) and ca. 820 Ma (C). Reconstructions are based mainly on paleolatitude of each block while fitting geological evidence. (B) Yangtze and North Tarim are separated from Cathaysia and South Tarim by Jiangnan–Central Tarim Ocean at ca. 900 Ma. Gray bars represent paleolatitude uncertainties for North Tarim and South Tarim. (C) Final closure of Jiangnan–Central Tarim Ocean and amalgamation of both South China and Tarim achieved between 870 and 820 Ma. All maps are in Mollweide projection.

the external margins of South China, Tarim, and Australia (Fig. 4C; Cawood et al., 2018). Furthermore, this Rodinia reconstruction agrees with the similarity of detrital zircon populations of Tarim, South China, and Australia–East Antarctica (Cawood et al., 2013). Our new paleomagnetic result and paleogeographic model thus provide spatiotemporal constraints on both the kinematics and dynamics of final Rodinia assembly. It was peripheral assembly along the northern margin of Rodinia that heralded the final amalgamation of the Neoproterozoic supercontinent.

ACKNOWLEDGMENTS

This research was supported by the National Nature Science Foundation of China (41888101). Zhao was supported by the Pioneer Hundred Talents Program of the Chinese Academy of Sciences. We thank the editor William Clyde for handling the manuscript. We appreciate Alan Collins, Conall Mac Niocaill, Joseph Meert, and an anonymous reviewer for critical review and revision of the manuscript. This work benefited from discussion with X.F. Liang.

REFERENCES CITED

Cawood, P.A., Wang, Y.J., Xu, Y.J., and Zhao, G.C., 2013, Locating South China in Rodinia and Gondwana: A fragment of greater India litho-

sphere?; *Geology*, v. 41, p. 903–906, <https://doi.org/10.1130/G34395.1>.

- Cawood, P.A., Zhao, G.C., Yao, J.L., Wang, W., Xu, Y.J., and Wang, Y.J., 2018, Reconstructing South China in Phanerozoic and Precambrian supercontinents: *Earth-Science Reviews*, v. 186, p. 173–194, <https://doi.org/10.1016/j.earscirev.2017.06.001>.
- Choudhary, B.R., Ernst, R.E., Xu, Y.G., Evans, D.A.D., de Kock, M.O., Meert, J.G., Ruiz, A.S., and Lima, G.A., 2019, Geochemical characterization of a reconstructed 1110 Ma Large Igneous Province: *Precambrian Research*, v. 332, 105382, <https://doi.org/10.1016/j.precamres.2019.105382>.
- Dalziel, I.W.D., 1997, Neoproterozoic–Paleozoic geography and tectonics: Review, hypothesis,

- environmental speculation: *Geological Society of America Bulletin*, v. 109, p. 16–42, [https://doi.org/10.1130/0016-7606\(1997\)109<0016:ONPGAT>2.3.CO;2](https://doi.org/10.1130/0016-7606(1997)109<0016:ONPGAT>2.3.CO;2).
- Enkin, R.J., 2003, The direction-correction tilt test: An all-purpose tilt/fold test for paleomagnetic studies: *Earth and Planetary Science Letters*, v. 212, p. 151–166, [https://doi.org/10.1016/S0012-821X\(03\)00238-3](https://doi.org/10.1016/S0012-821X(03)00238-3).
- Evans, D.A.D., 2013, Reconstructing pre-Pangean supercontinents: *Geological Society of America Bulletin*, v. 125, p. 1735–1751, <https://doi.org/10.1130/B30950.1>.
- He, B.Z., Jiao, C.L., Cai, Z.H., Zhang, M., and Gao, A.R., 2011, A new interpretation of the high aeromagnetic anomaly zone in central Tarim Basin: *Chinese Geology*, v. 38, p. 961–969 (in Chinese with English abstract).
- He, J.Y., Xu, B., and Li, D., 2019, Newly discovered early Neoproterozoic (ca. 900 Ma) andesitic rocks in the northwestern Tarim Craton: Implications for the reconstruction of the Rodinia supercontinent: *Precambrian Research*, v. 325, p. 55–68, <https://doi.org/10.1016/j.precamres.2019.02.018>.
- Hoffman, P.E., 1991, Did the breakout of Laurentia turn Gondwana inside out?: *Science*, v. 252, p. 1409–1412, <https://doi.org/10.1126/science.252.5011.1409>.
- Jing, X.Q., Yang, Z.Y., Evans, D.A.D., Tong, Y.B., Xu, Y.C., and Wang, H., 2020, A pan-latitudinal Rodinia in the Tonian true polar wander frame: *Earth and Planetary Science Letters*, v. 530, 115880, <https://doi.org/10.1016/j.epsl.2019.115880>.
- Li, Y.J., Song, W.J., Wu, G.Y., Wang, Y.F., Li, Y.P., and Zheng, D.M., 2005, Jinning granodiorite and diorite deeply concealed in the central Tarim Basin: *Science in China Series D: Earth Sciences*, v. 48, 2061, <https://doi.org/10.1360/03yd0354>.
- Li, Z.X., Zhang, L.H., and Powell, C.M., 1995, South China in Rodinia: Part of the missing link between Australia–East Antarctica and Laurentia?: *Geology*, v. 23, p. 407–410, [https://doi.org/10.1130/0091-7613\(1995\)023<0407:SCIRPO>2.3.CO;2](https://doi.org/10.1130/0091-7613(1995)023<0407:SCIRPO>2.3.CO;2).
- Li, Z.X., et al., 2008, Assembly, configuration, and break-up history of Rodinia: A synthesis: *Precambrian Research*, v. 160, p. 179–210, <https://doi.org/10.1016/j.precamres.2007.04.021>.
- Lin, S.F., Xing, G.F., Davis, D.W., Yin, C.Q., Wu, M.L., Li, L.M., Jiang, Y., and Chen, Z.H., 2018, Appalachian-style multi-terrane Wilson cycle model for the assembly of South China: *Geology*, v. 46, p. 319–322, <https://doi.org/10.1130/G39806.1>.
- McFadden, P.L., and McElhinny, M.W., 1990, Classification of the reversal test in palaeomagnetism: *Geophysical Journal of International*, v. 103, p. 725–729, <https://doi.org/10.1111/j.1365-246X.1990.tb05683.x>.
- Meert, J.G., Pivarunas, A.F., Evans, D.A.D., Pisarevsky, S.A., Pesonen, L.J., Li, Z.X., Elming, S.-Å., Miller, S.R., Zhang, S.H., and Salminen, J.M., 2020, The magnificent seven: A proposal for modest revision of the Van der Voo (1990) quality index: *Tectonophysics*, v. 790, 228549, <https://doi.org/10.1016/j.tecto.2020.228549>.
- Merdith, A.S., et al., 2021, Extending full-plate tectonic models into deep time: Linking the Neoproterozoic and the Phanerozoic: *Earth-Science Reviews*, v. 214, 103477, <https://doi.org/10.1016/j.earscirev.2020.103477>.
- Pisarevsky, S.A., Wingate, M.T.D., Powell, C.M., Johnson, S., and Evans, D.A.D., 2003, Models of Rodinia assembly and fragmentation, in Yoshida, M., et al., eds., *Proterozoic East Gondwana: Supercontinent Assembly and Breakup*: Geological Society [London] Special Publication 206, p. 35–55, <https://doi.org/10.1144/GSL.SP.2003.206.01.04>.
- Song, S.G., and Li, X.H., 2019, A positive test for the Greater Tarim Block at the heart of Rodinia: Mega-dextral suturing of supercontinent assembly: COMMENT: *Geology*, v. 47, e453, <https://doi.org/10.1130/G45470C.1>.
- Spencer, C.J., Roberts, N.M.W., and Santosh, M., 2017, Growth, destruction, and preservation of Earth's continental crust: *Earth-Science Reviews*, v. 172, p. 87–106, <https://doi.org/10.1016/j.earscirev.2017.07.013>.
- Wang, Y.J., Zhang, A.M., Cawood, P.A., Fan, W.M., Xu, J.F., Zhang, G.W., and Zhang, Y.Z., 2013, Geochronological, geochemical and Nd-Hf-Os isotopic fingerprinting of an early Neoproterozoic arc–back-arc system in South China and its accretionary assembly along the margin of Rodinia: *Precambrian Research*, v. 231, p. 343–371, <https://doi.org/10.1016/j.precamres.2013.03.020>.
- Watson, G.S., and Enkin, R.J., 1993, The fold test in paleomagnetism as a parameter estimation problem: *Geophysical Research Letters*, v. 20, p. 2135–2137, <https://doi.org/10.1029/93GL01901>.
- Wen, B., Evans, D.A.D., and Li, Y.X., 2017, Neoproterozoic paleogeography of the Tarim Block: An extended or alternative “missing-link” model for Rodinia?: *Earth and Planetary Science Letters*, v. 458, p. 92–106, <https://doi.org/10.1016/j.epsl.2016.10.030>.
- Wen, B., Evans, D.A.D., Wang, C., Li, Y.X., and Jing, X.Q., 2018, A positive test for the Greater Tarim Block at the heart of Rodinia: Mega-dextral suturing of supercontinent assembly: *Geology*, v. 46, p. 687–690, <https://doi.org/10.1130/G40254.1>.
- Wu, G.H., Yang, S.A., Meert, J.G., Xiao, Y., Chen, Y.Q., Wang, Z.C., and Li, X., 2020, Two phases of Paleoproterozoic orogenesis in the Tarim Craton: Implications for Columbia assembly: *Gondwana Research*, v. 83, p. 201–216, <https://doi.org/10.1016/j.gr.2020.02.009>.
- Xu, Z.Q., He, B.Z., Zhang, C.L., Zhang, J.X., Wang, Z.M., and Cai, Z.H., 2013, Tectonic framework and crustal evolution of the Precambrian basement of the Tarim Block in NW China: New geochronological evidence from deep drilling samples: *Precambrian Research*, v. 235, p. 150–162, <https://doi.org/10.1016/j.precamres.2013.06.001>.
- Yan, C.L., Shu, L.S., Faure, M., Chen, Y., and Huang, R.B., 2019, Time constraints on the closure of the Paleo–South China Ocean and the Neoproterozoic assembly of the Yangtze and Cathaysia blocks: Insight from new detrital zircon analyses: *Gondwana Research*, v. 73, p. 175–189, <https://doi.org/10.1016/j.gr.2019.03.018>.
- Yang, Z.Y., Sun, Z.M., Yang, T.S., and Pei, J.L., 2004, A long connection (750–380 Ma) between South China and Australia: Paleomagnetic constraints: *Earth and Planetary Science Letters*, v. 220, p. 423–434, [https://doi.org/10.1016/S0012-821X\(04\)00053-6](https://doi.org/10.1016/S0012-821X(04)00053-6).
- Yao, J.L., Cawood, P.A., Shu, L.S., and Zhao, G.C., 2019, Jiangnan Orogen, South China: A ~970–820 Ma Rodinia margin accretionary belt: *Earth-Science Reviews*, v. 196, 102872, <https://doi.org/10.1016/j.earscirev.2019.05.016>.
- Zhang, C.L., Zou, H.B., Li, H.K., and Wang, H.Y., 2013, Tectonic framework and evolution of the Tarim Block in NW China: *Gondwana Research*, v. 23, p. 1306–1315, <http://doi.org/10.1016/j.gr.2012.05.00>.
- Zhao, G.C., 2015, Jiangnan Orogen in South China: Developing from divergent double subduction: *Gondwana Research*, v. 27, p. 1173–1180, <https://doi.org/10.1016/j.gr.2014.09.004>.
- Zhao, J.H., Zhou, M.F., Yan, D.P., Zheng, J.P., and Li, J.W., 2011, Reappraisal of the ages of Neoproterozoic strata in South China: No connection with the Grenvillian orogeny: *Geology*, v. 39, p. 299–302, <https://doi.org/10.1130/G31701.1>.
- Zhao, P., Chen, Y., Zhan, S., Xu, B., and Faure, M., 2014, The Apparent Polar Wander Path of the Tarim block (NW China) since the Neoproterozoic and its implications for a long-term Tarim–Australia connection: *Precambrian Research*, v. 242, p. 39–57, <https://doi.org/10.1016/j.precamres.2013.12.009>.
- Zhu, W.B., Zheng, B.H., Shu, L.S., Ma, D.S., Wan, J.L., Zheng, D.W., Zhang, Z.Y., and Zhu, X.Q., 2011, Geochemistry and SHRIMP U–Pb zircon geochronology of the Korla mafic dykes: Constraints on the Neoproterozoic continental breakup in the Tarim Block, northwest China: *Journal of Asian Earth Sciences*, v. 42, p. 791–804, <https://doi.org/10.1016/j.jseaes.2010.11.018>.

Printed in USA